Proceedings of the 19th Conference on Computer Science and Intelligence Systems (FedCSIS) pp. 475–484
DOI: 10.15439/2024F4108
ISSN 2300-5963 ACSIS, Vol. 39

Towards crop traits estimation from hyperspectral data: evaluation of neural network models trained with real multi-site data or synthetic RTM simulations

Lorenzo Parigi
0000-0003-4641-7672
Institute for Electromagnetic Sensing of the Environment, National Research Council, 20133 Milan, Italy.
Department of Civil, Constructional and Environmental Engineering, Sapienza University of Rome, Rome, Italy
Email: parigi.l@irea.cnr.it

Gabriele Candiani
0000-0003-0575-068X
Institute for Electromagnetic Sensing of the Environment, National Research Council, 20133 Milan, Italy
Email: candiani.g@irea.cnr.it

Ignazio Gallo
0000-0002-7076-8328
Department of Theoretical and Applied Science, University of Insubria, 21100 Varese, Italy
ignazio.gallo@uninsubria.it

Piero Toscano
0000-0001-9184-0707
Institute of BioEconomy, National Research Council, 50145 Florence, Italy
piero.toscano@ibe.cnr.it

Mirco Boschetti
0000-0003-2156-4166
Institute for Electromagnetic Sensing of the Environment, National Research Council, 20133 Milan, Italy
boschetti.m@irea.cnr.it

***Abstract*—Hyperspectral images from newly launched (ASI-PRISMA and DLR-EnMAP) and future satellite (ESA-CHIME) are an opportunity, thanks to the high spectral resolution and full range continuity, to improve the retrieval of information about the crop parameters and status. The high dimensionality of hyperspectral data and the non-linear relationship between the crop biophysical parameters and their spectral signature make quantitative estimation of crop characteristics challenging, to address these problems we tested different configurations of neural networks (fully connected and convolutional). We tested the different architectures on two training dataset, one consists in ground data collected in three experiments, in different locations and seasons, the second one (hybrid) is composed by synthetic data generated using a radiative transfer model (PROSAIL-PRO). Preliminary results for LAI, CCC and CNC retrieval are encouraging in particular when ground data are exploited demonstrating of the potentiality of NN to fully exploit the information density of the hyperspectral data.**

***Index Terms*—Hyperspectral, Neural Network, RTM, PROSAIL, synthetic data, Wheat**

I. Introduction

IN THE pre-industrial period, worldwide production and consumption of food happened parallel to each other. Nowadays, the global megatrends (climate change, population growth, technological change) gradually caused the supply-demand balance to shift towards a not sufficient and unsustainable food production, with a potentially dramatic consequence for environmental and humanitarian aspects [1]. Considering this scenario, food-production system are forced to increase yields while protecting their most important production factors, soil from degradation, water and air from pollution and atmosphere from emissions of greenhouse gasses [2] as well as contributing to the mitigation of climate changes by increasing the carbon stock capability of agroecosystems.

To achieve such a goal, agriculture in the recent decades has increased the interest in collecting complex information about field status to better manage nutrients, water, chemicals [3] and tillage operations. For this scope geo-information products can be used to provide farmers with decision-supporting spatial information (crop traits maps), able to highlight within-field crop variability, as a fundamental tool to support site-specific management (i.e. precision farming) [1], [4]. Among the agro-practices supported by precision farming, nitrogen (N) fertilizations are fundamental, being nitrogen the most important limiting factor to crop growth together with water deficit. Overall, the nitrogen use efficiency in agriculture is estimated at 60%, with a negative effect on the sustainability of crop production from an economic and ecological point of view [5]. Excess nitrogen can be transformed into N_2O, which is a major contributor to climate change; in addition, it can be leached and reach water

The study was performed under the funding of the PNRR MUR – M4C2 (Mission 4 Component 2) Investment 1.4 "National Research Centre for Agricultural Technologies" Agritech, with project code CUP HUB – B63D21015240004.

masses, thus promoting eutrophication [6]. In order to rationalize the use of fertilizers in a smart agriculture paradigm, a deeper knowledge of the spatio-temporal dynamics of crops is required. Monitoring of this variability can be achieved through the use of data acquired from satellite earth observation systems able to produce maps of crop status at regular time.

In this framework, a great contribution is expected by hyperspectral remote sensing data able to provide continuous information to identify specific spectral features diagnostic of soil-plant compounds. New spaceborne image spectroscopy missions have been recently launched e.g. the PRISMA satellite, of the Italian Space Agency (ASI), and EnMAP of the German Space Agency (DLR) are already in orbit from 2019 and 2022 respectively. These systems are precursors able to provide contiguous, spectral sampling, from visible to shortwave infrared regions that covers ranges unobserved by multispectral data (400-2500 nm) and they are used by the scientific community to develop algorithm solutions for the future operational missions such as the CHIME (Copernicus Hyperspectral Imaging Mission for the Environment) of the European Space Agency's (ESA) [7].

A. From spectra to crop status information a complex task

Methods for quantitatively estimating the biophysical parameters (biopars) of plants from hyperspectral data are therefore required in order to generate space-time variability information to support agro-monitoring and management. Different biopars influence specific regions of the electromagnetic spectrum (e.g. Chlorophyll in the visible red-edge region 600-750 nm), but unfortunately several biopars can have a common influence on the same portion of the spectrum. For example, water, nitrogen, and carbon base constituent of leaves strongly influence the short wave infrared region around 1700 nm. Because of this, biopars retrieval from spectral data is not an easy task and classical statistical approaches can fail to provide reliable quantitative estimation, because the relationships are complex and very often non-linear [8], [9].

To overcome the problem of non-linearity and the interaction of the effect of different biopars on the spectrum, various machine learning algorithms have been proposed in the literature. In the field of machine learning, neural networks (NN) have achieved great popularity in recent years, they can be very effective in solving complex problems in both computer vision in agriculture [10] and quantitative estimation of environmental variable because they are able to achieve very good results even in the presence of non-linear relationships [11], [12]. Specifically, we focus on two NN architectures: fully connected networks (FC-NNs) and convolutional neural networks (CNNs). FC-NNs are straightforward to implement and suitable for tabular data. At the same time, CNNs, commonly used in image processing, can effectively capture local spectral features by applying convolutional filters across the spectral bands.

Another issue for the development of retrieval models is in general the small amount of actual ground vs spectral data on which the models should be trained. This scarcity is mainly due to the fact that it is expensive in terms of money and time to perform coupled sampling of biopars and spectroradiometric measurements from ground or contemporary to satellite overpass. Furthermore, the sampled data are representative of only the environment and conditions in the area, thus making it more difficult to export the results obtained with them to other contexts. To solve this problem, the use of methods that exploit physically based models is emerging in the literature; these radiative transfer models (RTMs) allow to simulate spectra from the leaf components and their arrangement in space. The advantage of RTMs is that they can simulate canopy spectral response even for diverse conditions that would be difficult to sample in the field. Once generated such a database of vegetation parameters (model input) and synthetic spectra (model output), machine learning algorithms can be trained to solve the problem. This method in literature is called hybrid and has been recently proposed in scientific literature as the state-of-the-art approach, as it combines the generic properties of RTMs with the flexibility and computational efficiency of machine learning regression algorithms, representing an innovative solution to the so-called inversion problem [11], [13], [14], [15], [16].

In this framework, the aim of this work is to test a machine learning solution to generate a retrieval model able to estimate crop biopar from hyperspectral data. More specifically the study wanted to generate a multi year/site database exploiting ground hyperspectral measurements acquired in different experiments together with corresponding bipolar measurements. This dataset was analyzed with different NN solutions in a ground data driven (using only experimental data) and hybrid approach (using RTM simulation). Different algorithm configurations have been tested, fully-connected (FC) and convolutional neural networks (CNN) to determine which architecture is the most effective. The long term perspective is to develop solutions for automatic estimation of quantitative crop information from new generation satellite data such as PRISMA and EnMAP.

II. Materials and Methods

A. Ground data

The experimental data used to test NN solutions have been acquired in the field in 2022 and 2023 from three different projects in 8 farms in Italy (Fig. 1).

We exploited data acquired with different purposes. A Field Phenotyping experiment (FP) was conducted in Arborea (Sardinia) in 2022. 4 different durum wheat varieties were cultivated in experimental plots of 6 m × 3 m with two types of soil preparation and 4 fertilization levels with three replicate for a total of 96 samples. Data were acquired three times during the season. Details of experiment and data acquisition can be found in [17].

Fig. 1: Position of the experiments

Field level Experiments (FE), devoted to set up a decision support system to support sowing density and fertilization management, were performed on 5 farms cultivated with soft wheat in the center-north of Italy in 2023. In each farm, one field was divided in 4 strips: the first representing the control (standard management following farm prescription), the second involves a reduction of nitrogen fertilization (-20%), the third reduction of seed density (-20%) and the last the combination of nitrogen and seeds reduction (-20% of both). Fields were monitored two times during the season at stem elongation and heading.

The Farm Monitoring experiment (FM) was conducted in Jolanda di Savoia (Ferrara) in Bonifiche Ferraresi estate in 2023. Wheat fields conditions were monitored acquiring data on four (10 by 10 m) plots in 10 elementary sampling units (ESU) for a total of 40 sampling sites. ESU were selected in different crop conditions defined according to analysis of previous year satellite data (within field anomaly from Sentinel 2 data) and on the base of the soil maps provided by the farm. 5 ESU were positioned in two fields cultivated with Durum and Soft Wheat respectively.

In all the farms, Leaf Area Index (LAI), Canopy Chlorophyll Content (CCC), and Canopy Nitrogen Content (CNC) were collected following [16] approach. LAI, which measures the one-sided green leaf area per unit of ground surface, is a crucial canopy trait as it describes vegetation density and regulates carbon, energy, and water fluxes in terrestrial ecosystems. Quantifying CCC is essential for monitoring photosynthetic efficiency and the early detection of crop stress, such as chlorosis. CNC is a direct estimation of plant nitrogen uptake fundamental to support smart fertilization strategy.

Proximal spectral measurements were acquired using a handheld spectrometer (Spectral Evolution) with full spectral range (350-2500 nm) capacity and 3 nm spectral sampling interval (SSI). Spectral measurements were conducted per each plot approximately 1 m above the canopy with a nadir viewing angle and under clear sky conditions with multiple replicates. Before the target measurements, the radiance of a reference panel was collected to derive the top of canopy reflectance for each replicate, then the plot average value was calculated. The ground spectra were resampled to match the PRISMA configuration, encompassing a spectral range from 400 to 2500 nm with an average SSI of less than 10 nm. This resampling process resulted in a total of 230 spectral bands, utilizing Gaussian spectral response functions (SRF) generated based on the center wavelengths and full-width-half-maximum values of PRISMA bands. Spectral regions between 1328-1491 nm and 1794-1993 nm and the last portion of the SWIR between 2378-2500 nm were excluded resulting in a total of 170 so-called PRISMA-like spectral bands. The final goal is to transfer the retrieval models to actual PRISMA images to produce biopars' maps to investigate crop status conditions in space and time.

The ground data from the three experiments is combined in a single database composed by the biopars' values and the corresponding measured reflectance for the 170 PRISMA-like spectral bands. We split all the data in train, validation and test set, our objective was to generate the most representative validation and test sets by assuring, if possible, that all the combinations produced in the different experiments were present in both. The number of biopar-spectra couples is shown in I.

B. Simulated data from RTM

The initial step of a hybrid approach, which involves training a machine learning algorithm with synthetic data, is therefore the generation of the Look Up Table (LUT) of synthetic spectra and corresponding input parameters. The PROSAIL model has been widely used to obtain plant biochemical and structural variables in the agricultural context [18]. The hybrid approach combines the PROSPECT leaf model [19] and the 4SAIL canopy model [20]. The PROSPECT-PRO is the latest version of PROSPECT which was introduced to differentiate specific absorption coefficients of carbon-based (CBC) and protein (CP) leaf constituents. The 4SAIL model requires as input the leaf reflectance and transmittance generated from PROSPECT as well as canopy density information (i.e., LAI), leaf orientation (average leaf angle, ALA), background spectral properties (i.e. soil reflectance) and the illumination and viewing angles (i.e. sun-sensor-target geometry). The resulting combined model (PROSAIL-PRO [21]) is able to simulate reflectance spectra at canopy level as it would be recorded by a remote sensor (i.e. satellite system).

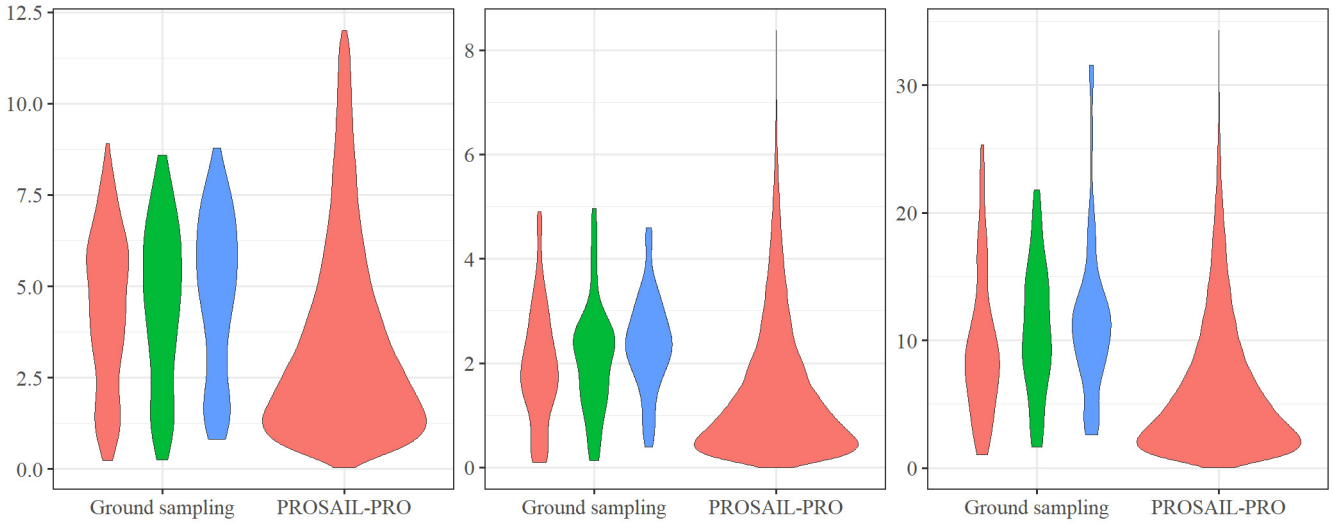

Fig. 2: Distribution of the parameters LAI [m^2 m^{-2}], CCC [g m^{-2}], and CNC [g m^{-2}] (from left to right) and their split in training (red), validation (green) and test (blue) sets.

The simulation was performed using a MATLAB script of [15] which i) couples the two models and ii) generates distributions of input variables. The generation of the LUT represents a critical step, as it should be representative of vegetation reflectance spectra, including a-priori information on the ranges and distribution of the input variables [22]. To prevent unrealistic combinations of these variables, the method exploits covariances between certain vegetation traits acquired during several field campaigns. The probability density functions (PDFs) and the related ranges used in the simulation have been selected according to actual measured values. The remaining values were selected according to literature or authors' experience as reported in [15]. The script was used to simulate 50000 reflectance spectra from plausible combinations of crop traits. As shown in Fig. 2, the distribution of the parameters used to generate the reflectance spectra is larger then the sampled records, allowing us to train the model on a more extensive and complete dataset with combination that could not be sampled in our working zones. A subsamples based on different LAI levels is shown in Fig. 3.

C. *Neural networks*

In this study, we employed two neural network architectures: fully connected neural networks (FC-NNs) and convolutional neural networks (CNNs). The choice of these architectures was driven by their distinct capabilities in handling the characteristics of hyperspectral data:

- FC-NNs are a fundamental type of neural network where each neuron is connected to every other neuron in the subsequent layer. This architecture is straightforward and efficient for handling structured data, such as the resampled spectral measurements we obtained. FC-NNs can capture complex, global relationships between input features (spectral bands) and output variables (crop parameters). In our implementation, this architecture is composed by a sequence of FC blocks (FCb), where each FCb is composed by a linear (or fully connected) layer followed by a ReLU activation function and a dropout layer.
- CNNs are particularly effective in processing data with spatial hierarchies, making them well-suited for image and spectral data. By applying convolutional filters, CNNs can capture local patterns and

Table I: Number of biopar-spectra couple. *FF = Field plot level Phenotyping experiment, FE = Field level Experiment, FC =Farm level Monitoring experiment. ** DW = Durum Wheat, SW = Soft Wheat

Study*	Crop**	Training			Validation			Test		
		LAI	CCC	CNC	LAI	CCC	CNC	LAI	CCC	CNC
FP	DW	141	36	27	69	18	12	66	18	12
FM	SW	59	59	59	24	24	24	20	20	20
FE	DW and SW	36	36	35	14	14	14	14	14	11
Total		236	131	121	107	56	50	100	52	43

Table II: Ranges or steps of the hypermarameters

Hyperparameter	Range
Batch size	16, 32, 64, 128
Learning rate	0.1-0.0001
N. of FCb	1-5
N. of CNNb	0-4
Dropout in the FCb	0-0.5 (by 0.05)
Dropout in the CNNb	0-0.5 (by 0.05)
N. of output neurons of the FCb	16, 32, 64, 128, 256, 512
N. of output channels of the CNNb	4, 8, 16, 32
Kernel size of the CNNb	3, 5, 7

spectral features across bands, which is crucial for identifying subtle variations in hyperspectral data that correspond to different crop traits. The hierarchical feature extraction in CNNs enables a more nuanced understanding of the spectral signatures, potentially leading to better performance in crop parameter estimation. In our implementation, the CNN is a sequence of Convolutional blocks (CNNb) and FCb, where each CNNb is composed by two 1D convolutional layer both followed by a ReLU function and stacked together, followed by a dropout layer and a Max Pooling layer.

We tested 100 different models with different hyperparametrization. The hyperparameters that change between each model are: batch size, learning rate, number of FCb, number of CNNb, dropout in the FCb (d) and in the CNNb (d), number of neurons in the FCb (n_out), number of output channel in the convolutional layers (c_out), and the kernel size of the convolutional layers (k). The ranges of those hyperparameters are described in the II and in Fig. 4 is showed the blocks' architecture. The shape of input data is [B, 170] for the FC architecture and [B, 1, 170] for the CNN architecture, where B is the batch size. The stride (s) of the CNN layers is always 1, the padding value (p) depends on the k value and it is obtained by the integer division of k by 2. The k and s values of the max pool layer is 2 for both.

Given this hyperparametrization strategy, 19 out of 100 models present only FC layers, the remaining present at least one CNNb.

The number of epochs in the training phase was set to 3000 for data driven FC NN, 1000 for the data driven CNN, for the hybrid models 300 and 100 for FC NN and CNN, respectively. The models with the best Mean Squared Error (MSE) on the validation set were selected during the training without reaching the maximum epoch number, then they were used to predict on the test data.

Following the training phase, the top-performing models were assessed on the test dataset. The correlation between observed and estimated data was evaluated using the coefficient of determination (R^2) of linear regression, while the retrieval error was quantified by calculating the Root Mean Squared Error (RMSE) and the relative RMSE (rRMSE) as follows:

$$RMSE = \sqrt{\frac{1}{n}\sum_{i=1}^{n}(x_i - y_i)^2} \quad (1)$$

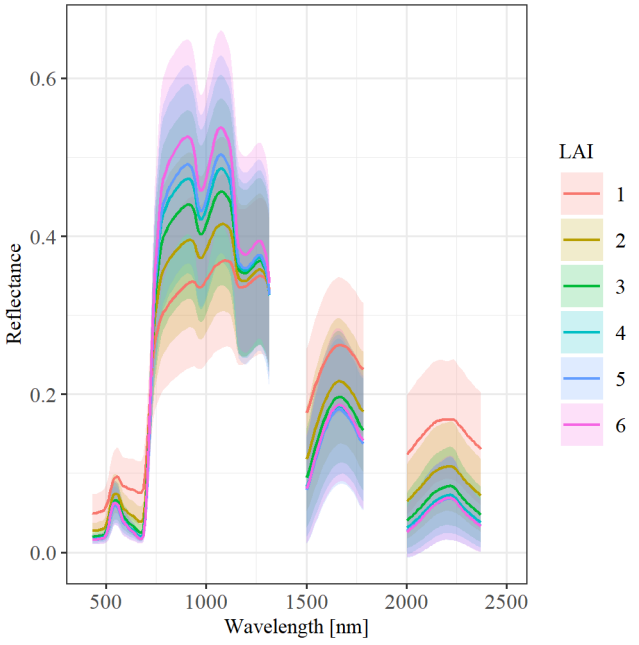

Fig. 3: Examples of synthetic hyperspectral signature. The line represent the reflectance mean and the semi-transparent zone is the standard deviation

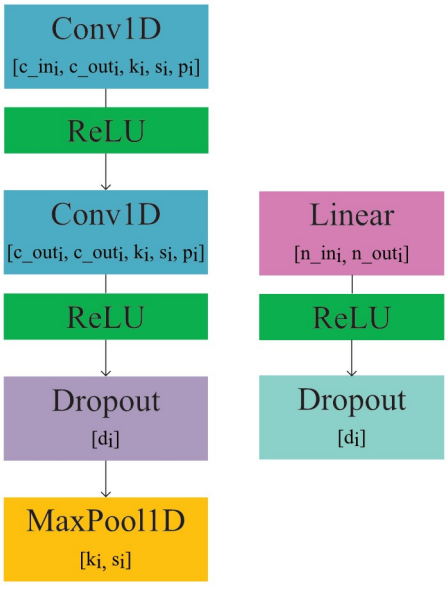

Fig. 4: Description of the convolutional block (CNNb) on the left and the fully connected block (FCb) on the right. Where c_in and c_out are the input and output size of the CNNs, k, s and p are the kernel, stride and padding size, respectively. n_in and n_out are the FC dimensions. d is the dropout value. The subscript i is the model number.

$$rRMSE = \frac{RMSE}{y_{max} - y_{min}} \quad (2)$$

Where x_i and y_i are respectively the i-th sample of the predicted and actual values, y_{max} and y_{min} are the max and min value of the observed parameters, respectively.

III. Results and Discussion

Results for the best ten models, for the three considered biopar (LAI, CCC and CNC) are reported in III, IV, and V together with details of adopted hyperparametrization. Fig. 5, Fig. 6, and Fig. 7 shows the scatter plot of actual vs predicted biopar (LAI, CCC and CNC) for the first five best models reporting regression line for the different dataset (FP, FM, FE).

Models for LAI retrieval (Fig. 5 and III) produced very satisfying results with a R2, between observed and predicted values, up to 0.73 and a rRMSE below 12%. Regarding the tested retrieval methods, the data-driven approach (RMSE = 0.962) outperforms the hybrid approach (RMSE = 1.209) on average, demonstrating a 25% reduction in retrieval error.

The primary distinction between the hybrid and data-driven approaches in the LAI estimation lies in the differing numbers of models that incorporate at least one CNNb. Among the top 10 data-driven models, only three contain one or two CNNb. Furthermore, the first three models are all FC NNs and among them the first two have only one FC layer with 256 and 64 neurons, respectively. Conversely, for the hybrid 7 models with at least one CNNb were selected for the top 10. This aspect may be attributed to the quantity of data employed during the training phase. More complex models, incorporating multiple CNNb and/or deeper architecture, demonstrate superior performance in hybrid approach. This is likely because these model can extract most diagnostic features when trained with 50,000 samples by PROSAIL simulation.

The models for the estimation of CCC (Fig. 6 and IV)produced moderate results in term or correlation between estimates and observation ($R^2 < 0.5$). Once again, the results are superior when the model are trained on field data, with an average RMSE of 0.616 (rRMSE < 15%). However, the scatterplots of Fig. 6 show discrepancies between the experiments, with the FE experiment poorly predicted. On the other hand, in the hybrid approach the FM and FE experiments tend to be more in accordance, instead the FP deviates the most from the 1:1 line. Due to the larger CCC range of FP, the average value of R^2 for hybrid scenario (0.259) is lower than the data driven one (0.471). However, the difference in term of RMSE is only of 13.6% between the best models of the two approaches. Despite the dispersion in the hybrid models, the values tend to cluster by experiment, resulting in relatively tight groupings around their respective trend lines highlighting a possible bias in the ground measurements. In the CCC estimation, both approaches have 5 FC NN models and 5 CNN models in the top 10 best.

The performance of the CNC models (Fig. 7 and V) is similar to the CCC one; however, the values are more scattered, leading to moderate model performance ($R^2 < 0.54$). Additionally, no single experiment consistently outperforms the others. Moreover, the CNC performed slightly worse than CCC in terms of the average rRMSE for both data driven (15.62% vs 17.98%) and hybrid (17.74% vs 18.93%) approaches. The data driven approach produced again better results in term of RMSE (3.270) relatively to the hybrid (3.442), but with a narrower difference of only 5.3%. Despite this negative aspects, it is encouraging that model retrieval are always in the range of the observed values even when hybrid model is used. Moreover, an rRMSE below 20% is an encouraging result, considering the uncertainty of ground measurements in real farming conditions. Similar to the LAI results, 9 of the top 10 hybrid models contain at least one CNNb, compared to only 4 in the data-driven approach.In comparison to the other biopars, LAI exhibits the most significant difference between data driven and hybrid approaches in term of RMSE. This discrepancy may be attributed to the larger number of samples on which training have been performed, which enhances the model's capacity to predict field data. Conversely, the estimates of CCC and CNC exhibit a smaller decline in performance when utilizing the hybrid approach. This behavior may be caused by the reduced number of training samples, which may have negatively impacted the performance of the data driven models but candidate hybrid approach as a solution when few data are available. Indeed, the rRMSE of the hybrid models present small variations between LAI, CCC and CNN (in order: 15.65%, 17.74%, 18.93%), underlying a good stability across the biopars estimation that can be used as a starting point when the field data are lacking.

The results are overall encouraging and there are margins of improvements in both data driven and hybrid approaches. The hybrid models tend to perform worse than the data driven ones, but they are promising, especially when the number of samples are relatively small. In this case the generation of spectra through an RTM allows the training of models with good predictive performance on field data that are totally independent hence candidate this model to be more exportable in different situation and data input. Among the biopars analyzed, CNC is the one that has an important agronomic relevance, because the possibility of creating spatio-temporal estimation of plant nitrogen from satellite data is a determining factor in supporting site specific nitrogen fertilization scheduling by producing digital prescription maps. Nitrogen sampling and measurements in field is more labor-intensive than LAI and CCC, consequently the fact that CNC can be estimated using radiometric tools (on ground or from remote) and hybrid models can represent a feasible solution to facilitate smart and more rational crop fertilization dosing.

Table III: Hyperparametrization of the 10 best data driven and hybrid models for the estimation of LAI and their predictive performance. Results are in descending other from best to worst in term of RMSE. CNN model are highlighted in grey

Data driven

CNNb	FCb	CNN channels	FC neurons	RMSE	R^2	rRMSE
0	1	[0]	[256]	0.923	0.725	11.94%
0	1	[0]	[64]	0.933	0.696	12.07%
0	4	[0]	[512,32,64,16]	0.959	0.721	12.41%
1	2	[4]	[32,128]	0.962	0.681	12.45%
0	4	[0]	[64,64,256,32]	0.964	0.703	12.47%
0	3	[0]	[32,32,256]	0.966	0.678	12.50%
0	1	[0]	[16]	0.967	0.691	12.51%
0	4	[0]	[16,128,128,32]	0.98	0.662	12.68%
1	3	[4]	[16,16,16]	0.981	0.673	12.69%
2	3	[16,4]	[32,32,256]	0.984	0.671	12.73%
			Mean	0.962	0.690	12.44%

Hybrid

CNNb	FCb	CNN channels	FC neurons	RMSE	R^2	rRMSE
1	2	[4]	[64,512]	1.144	0.519	14.80%
1	1	[16]	[512]	1.168	0.497	15.11%
4	2	[4,16,16,8]	[64,256]	1.182	0.509	15.29%
2	3	[8,8]	[256,16,64]	1.201	0.510	15.54%
1	4	[4]	[512,256,128,512]	1.216	0.460	15.73%
0	3	[0]	[32,32,256]	1.225	0.454	15.85%
1	5	[32]	[64,64,32,256,256]	1.235	0.439	15.98%
2	2	[32,16]	[128,32]	1.238	0.463	16.02%
0	5	[0]	[64,512,256,512,512]	1.242	0.441	16.07%
0	5	[0]	[64,32,256,16,512]	1.243	0.484	16.08%
			Mean	1.209	0.478	15.65%

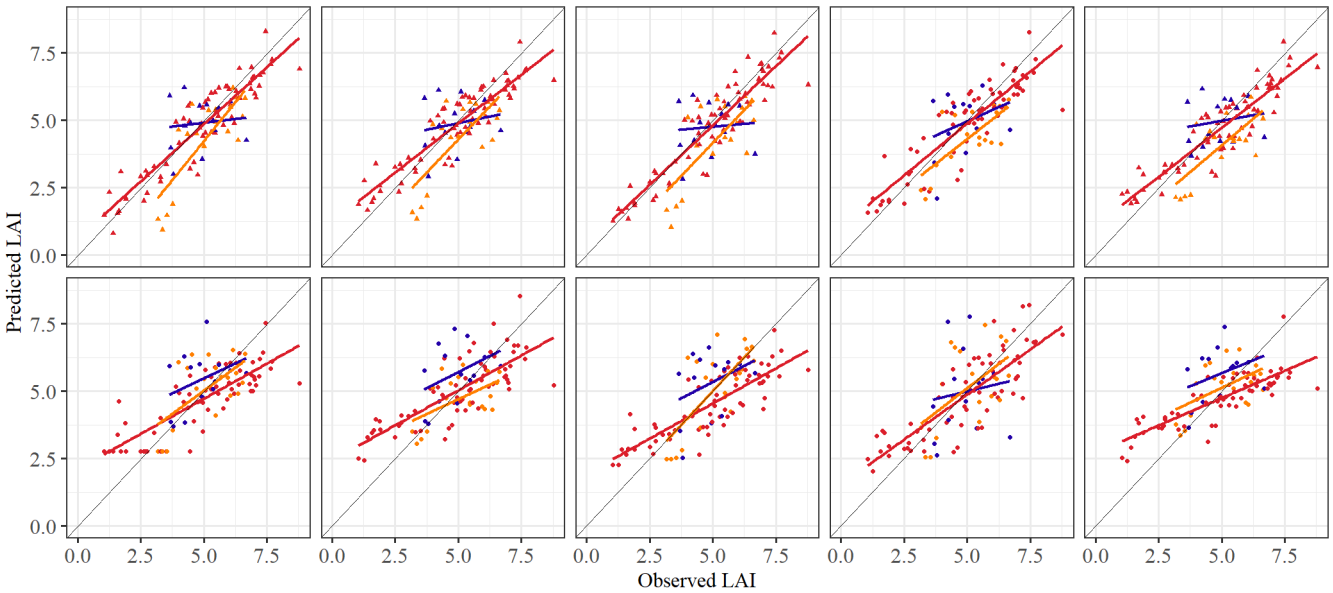

Fig. 5: Scatterplot between actual and predicted values of LAI of the 5 best data driven (top) and hybrid (bottom) models. The color represent the experiment FP (Orange), FM (Red), and FE (Blue). The 1:1 line is black, the other are the tendency lines colored by experiment. The FC NN models are represented by triangles and CNN ones by circles

Table IV: Hyperparametrization of the 10 best data driven and hybrid models for the estimation of CCC and their predictive performance. Results are in descending other from best to worst in term of RMSE. CNN model are highlighted in grey

Data driven

CNNb	FCb	CNN channels	FC neurons	RMSE	R^2	rRMSE
0	5	[0]	[64,512,256,512,512]	0.616	0.470	14.66%
0	3	[0]	[256,64,64]	0.623	0.468	14.83%
0	3	[0]	[32,32,256]	0.638	0.514	15.19%
1	4	[32]	[256,16,128,64]	0.639	0.488	15.21%
1	2	[16]	[512,64]	0.648	0.437	15.43%
0	4	[0]	[16,512,512,512]	0.664	0.405	15.81%
2	2	[8,32]	[512,32]	0.671	0.489	15.97%
0	5	[0]	[128,256,512,256,64]	0.684	0.503	16.28%
1	2	[16]	[512,64]	0.687	0.501	16.35%
1	2	[16]	[256,256]	0.69	0.440	16.43%
			Mean	0.656	0.471	15.62%

Hybrid

CNNb	FCb	CNN channels	FC neurons	RMSE	R^2	rRMSE
1	2	[16]	[512,64]	0.711	0.298	16.93%
0	5	[0]	[64,512,256,512,512]	0.725	0.264	17.26%
0	4	[0]	[16,512,512,512]	0.728	0.287	17.33%
0	3	[0]	[32,32,256]	0.74	0.261	17.62%
0	5	[0]	[64,32,256,16,512]	0.747	0.261	17.78%
2	5	[16,8]	[256,64,512,16,128]	0.749	0.235	17.83%
2	4	[8,16]	[512,128,128,128]	0.756	0.273	18.00%
0	5	[0]	[128,32,512,16,128]	0.759	0.218	18.07%
1	2	[16]	[128,16]	0.767	0.249	18.26%
1	2	[16]	[512,64]	0.769	0.239	18.31%
			Mean	0.745	0.259	17.74%

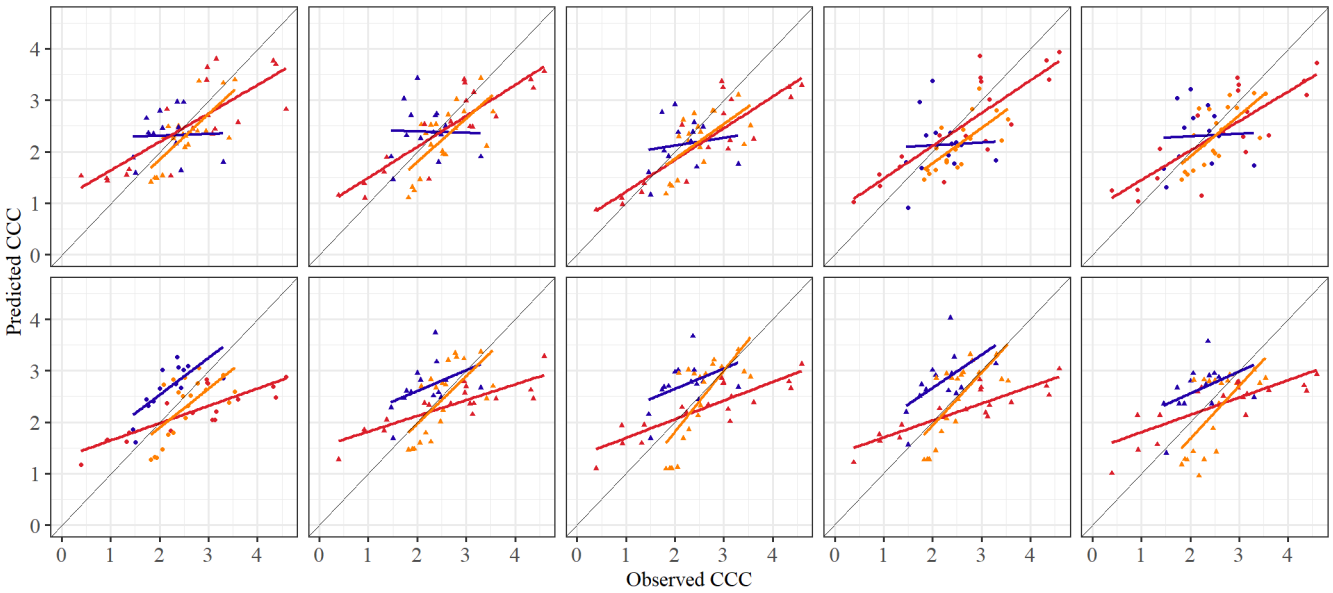

Fig. 6: Scatterplot between actual and predicted values of CCC of the 5 best data driven (top) and hybrid (bottom) models. The color represent the experiment FP (Orange), FM (Red), and FE (Blue). The 1:1 line is black, the other are the tendency lines colored by experiment. The FC NN models are represented by triangles and CNN ones by circles

Table V: Hyperparametrization of the 10 best data driven and hybrid models for the estimation of CNC and their predictive performance. Results are in descending other from best to worst in term of RMSE. CNN model are highlighted in grey

Data driven

CNNb	FCb	CNN channels	FC neurons	RMSE	R^2	rRMSE
0	5	[0]	[64,32,256,16,512]	2.837	0.542	15.60%
3	4	[4,8,16]	[16,32,32,16]	3.232	0.364	17.77%
0	4	[0]	[16,512,512,512]	3.25	0.388	17.87%
1	5	[8]	[256,32,128,32,16]	3.281	0.421	18.04%
0	3	[0]	[32,32,256]	3.288	0.467	18.08%
1	4	[8]	[64,16,32,256]	3.328	0.452	18.30%
0	1	[0]	[256]	3.348	0.357	18.41%
0	4	[0]	[16,128,128,32]	3.364	0.492	18.50%
1	2	[4]	[128,512]	3.385	0.459	18.61%
0	1	[0]	[16]	3.388	0.443	18.63%
			Mean	3.270	0.438	17.98%

Hybrid

CNNb	FCb	CNN channels	FC neurons	RMSE	R^2	rRMSE
4	5	[32,4,8,32]	[64,32,16,512,128]	3.114	0.366	17.12%
1	5	[32]	[64,64,32,256,256]	3.216	0.313	17.68%
1	1	[16]	[16]	3.359	0.346	18.47%
1	2	[16]	[128,16]	3.409	0.353	18.74%
2	4	[8,16]	[512,128,128,128]	3.52	0.296	19.35%
0	5	[0]	[64,512,256,512,512]	3.538	0.262	19.45%
1	2	[32]	[32,512]	3.543	0.390	19.48%
2	4	[8,4]	[16,256,512,512]	3.562	0.291	19.58%
1	4	[4]	[512,256,128,512]	3.576	0.240	19.66%
2	2	[8,32]	[512,32]	3.587	0.312	19.72%
			Mean	3.442	0.317	18.93%

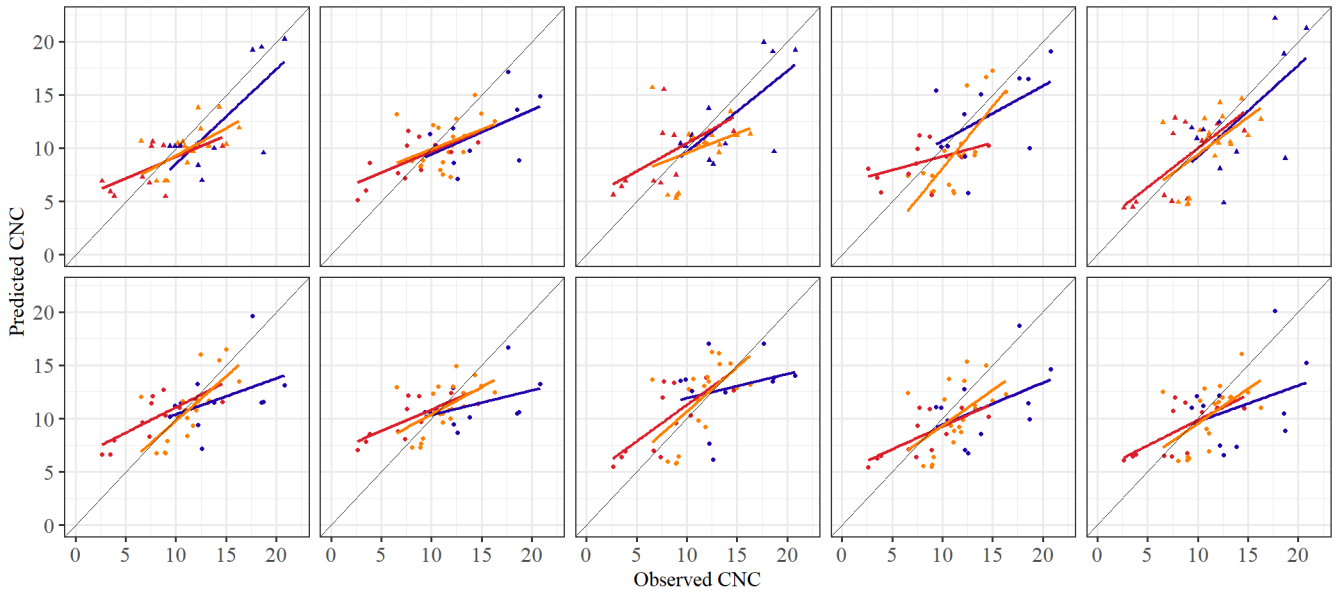

Fig. 7: Scatterplot between actual and predicted values of CNC of the 5 best data driven (top) and hybrid (bottom) models. The color represent the experiment FP (Orange), FM (Red), and FE (Blue). The 1:1 line is black, the other are the tendency lines colored by experiment. The FC NN models are represented by triangles and CNN ones by circles

IV. Conclusion and future perspective

The dataset involved in this work come from different location and was sampled by different operators. Integrating different datasets is challenging, as cardinality is not the only crucial factor; data quality and consistency in data collection and measurement protocols are also fundamental. In future work, the quality of individual datasets must be evaluated, and outliers and anomalous values must be assessed. Additionally, a deeper analysis of plant samples and measurement protocols is necessary. New data from ongoing experiment conduced in 2024 will be tested to assess the exportability of the obtained models on an independent data set and to train new model on increased datasets.

To refine the hybrid model's performance active learning and transfer learning techniques on field data will be explored. Finally, models trained with ground data will be tested on actual satellite data to validate their applicability to spaceborne sensors. The integration of the ground and satellite information, along with RTM simulations will be evaluated for an advanced retrieval scheme.

Acknowledgment

We thanks Dr. Ramin Heidarian Dehkordi for preparing the FP dataset acquired in 2022 in Sardinia and Dr. Riccardo Dainelli for the acquisition of data in the FE condition in 2023.

References

[1] T. B. Hank *et al.*, "Spaceborne Imaging Spectroscopy for Sustainable Agriculture: Contributions and Challenges," *Surv. Geophys.*, vol. 40, no. 3, pp. 515–551, May 2019, doi: 10.1007/s10712-018-9492-0.

[2] FAO, Ed., *The state of food and agriculture - Climate change, agriculture and food security*. in The state of food and agriculture, no. 2016. Rome: FAO, 2016.

[3] M. Wójtowicz, A. Wójtowicz, and J. Piekarczyk, "Application of remote sensing methods in agriculture," 2016.

[4] P. J. Zarco-Tejada, N. Hubbard, and P. Loudjani, "Precision agriculture: an opportunity for EU farmers: potential support with the CAP 2014-2020," 2014.

[5] L. Lassaletta *et al.*, "Nitrogen use in the global food system: past trends and future trajectories of agronomic performance, pollution, trade, and dietary demand," *Environ. Res. Lett.*, vol. 11, no. 9, p. 095007, Sep. 2016, doi: 10.1088/1748-9326/11/9/095007.

[6] S. M. Ogle, K. Butterbach-Bahl, L. Cardenas, U. Skiba, and C. Scheer, "From research to policy: optimizing the design of a national monitoring system to mitigate soil nitrous oxide emissions," *Curr. Opin. Environ. Sustain.*, vol. 47, pp. 28–36, Dec. 2020, doi: 10.1016/j.cosust.2020.06.003.

[7] K. Berger *et al.*, "Crop nitrogen monitoring: Recent progress and principal developments in the context of imaging spectroscopy missions," *Remote Sens. Environ.*, vol. 242, p. 111758, Jun. 2020, doi: 10.1016/j.rse.2020.111758.

[8] P. J. Curran, "Remote sensing of foliar chemistry," *Remote Sens. Environ.*, vol. 30, no. 3, pp. 271–278, Dec. 1989, doi: 10.1016/0034-4257(89)90069-2.

[9] Y. Fu *et al.*, "An overview of crop nitrogen status assessment using hyperspectral remote sensing: Current status and perspectives," *Eur. J. Agron.*, vol. 124, p. 126241, Mar. 2021, doi: 10.1016/j.eja.2021.126241.

[10] G. Castellano, P. D. Marinis, and G. Vessio, "Applying Knowledge Distillation to Improve Weed Mapping With Drones," presented at the 18th Conference on Computer Science and Intelligence Systems, Sep. 2023, pp. 393–400. doi: 10.15439/2023F960.

[11] J. Verrelst *et al.*, "Quantifying Vegetation Biophysical Variables from Imaging Spectroscopy Data: A Review on Retrieval Methods," *Surv. Geophys.*, vol. 40, no. 3, pp. 589–629, May 2019, doi: 10.1007/s10712-018-9478-y.

[12] I. Gallo, M. Boschetti, A. U. Rehman, and G. Candiani, "Self-Supervised Convolutional Neural Network Learning in a Hybrid Approach Framework to Estimate Chlorophyll and Nitrogen Content of Maize from Hyperspectral Images," *Remote Sens.*, vol. 15, no. 19, p. 4765, Sep. 2023, doi: 10.3390/rs15194765.

[13] M. Weiss, F. Jacob, and G. Duveiller, "Remote sensing for agricultural applications: A meta-review," *Remote Sens. Environ.*, vol. 236, p. 111402, Jan. 2020, doi: 10.1016/j.rse.2019.111402.

[14] K. Berger *et al.*, "Retrieval of aboveground crop nitrogen content with a hybrid machine learning method," *Int. J. Appl. Earth Obs. Geoinformation*, vol. 92, p. 102174, Oct. 2020, doi: 10.1016/j.jag.2020.102174.

[15] G. Candiani *et al.*, "Evaluation of Hybrid Models to Estimate Chlorophyll and Nitrogen Content of Maize Crops in the Framework of the Future CHIME Mission," *Remote Sens.*, vol. 14, no. 8, p. 1792, Apr. 2022, doi: 10.3390/rs14081792.

[16] G. Tagliabue *et al.*, "Hybrid retrieval of crop traits from multi-temporal PRISMA hyperspectral imagery," *ISPRS J. Photogramm. Remote Sens.*, vol. 187, pp. 362–377, May 2022, doi: 10.1016/j.isprsjprs.2022.03.014.

[17] R. Heidarian Dehkordi *et al.*, "Towards an Improved High-Throughput Phenotyping Approach: Utilizing MLRA and Dimensionality Reduction Techniques for Transferring Hyperspectral Proximal-Based Model to Airborne Images," *Remote Sens.*, vol. 16, no. 3, p. 492, Jan. 2024, doi: 10.3390/rs16030492.

[18] K. Berger, Z. Wang, M. Danner, M. Wocher, W. Mauser, and T. Hank, "Simulation of Spaceborne Hyperspectral Remote Sensing to Assist Crop Nitrogen Content Monitoring in Agricultural Crops," in *IGARSS 2018 - 2018 IEEE International Geoscience and Remote Sensing Symposium*, Valencia: IEEE, Jul. 2018, pp. 3801–3804. doi: 10.1109/IGARSS.2018.8518537.

[19] J.-B. Féret, "PROSPECT-PRO for estimating content of nitrogen-containing leaf proteins and other carbon-based constituents," *Remote Sens. Environ.*, 2021.

[20] W. Verhoef, "Light Scattering by Leaf Layers with Application to Canopy Reflectance Modeling: The SAIL Model," 1984.

[21] J.-B. Féret and F. de Boissieu, *prosail: PROSAIL leaf and canopy radiative transfer model and inversion routines*. 2023. [Online]. Available: https://gitlab.com/jbferet/prosail

[22] M. Weiss, S. Jay, and F. Baret, "S2ToolBox Level 2 products: LAI, FAPAR, FCOVER - Version 1.1.," 2016.